

Diagnostic Properties of Phytoplankton Time Series from Remote Sensing

Trevor Platt · Shubha Sathyendranath ·
George N. White III · César Fuentes-Yaco ·
Li Zhai · Emmanuel Devred · Charles Tang

Received: 19 August 2008 / Revised: 5 February 2009 / Accepted: 28 March 2009
© Coastal and Estuarine Research Federation 2009

Abstract Remote sensing provides our only window into the phytoplankton community on synoptic scales, permitting the construction of spatially distributed time series of biomass indexed as chlorophyll concentration. Data from the SeaWiFS mission have accumulated to the point where they meet the criterion of a 10-year series. The seasonal phytoplankton cycle is the dominant mode of temporal variability. The time series can be used to construct a variety of ecological indicators of the pelagic system useful in ecosystem-based management. These are reviewed and examples of their implementation are presented. Phenology of phytoplankton blooms is given particular attention. Interannual variation in some of the indicators is strong, presumably a response to variation in large-scale forcing. Examination of the results in the context of a simple phytoplankton-

nutrient model enhances the interpretation. Remote sensing imagery also lends itself to the retrieval of information on community structure, in addition to biomass. More information will be recovered from satellite imagery if the remote-sensing program is coupled closely to a ship program on which appropriate bio-optical observations are made. The data series can be distilled to yield concise descriptions of the unfolding of ecosystem characteristics through time.

Keywords Ecological indicators · Phytoplankton · Ocean colour · Remote sensing · Phenology

Introduction

The integrity of the marine ecosystem is maintained only by a regular input of energy from the sun. Capture of that solar input is possible by virtue of the pigment molecules contained in phytoplankton. The synoptic field of phytoplankton distribution, obtained, for example, by remote sensing of ocean colour and indexed as concentration of chlorophyll, can then be interpreted as a map of the coupling of the marine ecosystem to its energy source. It therefore represents the base of the marine food chain in the most fundamental sense. The map will vary quantitatively with region and season, and there will be a qualitative variability on the same time scales, associated with the seasonal succession of flora and the regional changes of physical forcing. When the synoptic maps are accumulated as a time series, they provide an invaluable chronology of the autotrophic community, its fluctuations within and between years in abundance, growth, loss, community structure and large-scale organisation.

This work was supported by the Canadian Space Agency (GRIP and EOPI programmes) and by Discovery Grants to TP and SS from the Natural Sciences and Engineering Research Council of Canada. This work is also a contribution to the NCEO and Oceans 2025 programmes of the Natural Environment Research Council (UK).

T. Platt · S. Sathyendranath
Plymouth Marine Laboratory, Prospect Place, The Hoe,
PL1 3DH, Plymouth, UK

T. Platt · G. N. White III (✉) · C. Tang
Coastal Ocean Science, Bedford Institute of Oceanography,
Dartmouth, Nova Scotia, B2Y 4A2, Canada
e-mail: gnwiii@gmail.com

T. Platt
e-mail: tplatt@dal.ca

C. Fuentes-Yaco · L. Zhai · E. Devred
Oceanography Department, Dalhousie University,
Halifax, Nova Scotia, B3H 4J1, Canada

The digital history represented in the maps contains an enormous body of information. It is important to find constructive ways to help in digestion and synthesis. Platt and Sathyendranath (2008) have shown how the data can be used to extract a suite of ecological indicators that would provide an economical and informative history of the pelagic ecosystem. The indicators are objective metrics that can be applied or extracted serially to detect possible modifications to ecosystem properties under perturbations, either natural or man-made.

Visible spectral radiometry of the ocean conducted remotely by instruments carried on polar-orbiting spacecraft, yields the required ocean-colour fields with excellent resolution in time and space (nominally 2 days and 1 km). The SeaWiFS mission has already accumulated a data stream of more than 10 years in length. Here, we examine data from this series, supplemented by remotely sensed sea-surface temperature (SST), for the continental shelf of the Northwest Atlantic Ocean, and illustrate the application of the derived ecological indicators to elucidate the regional structure of the pelagic ecosystem, its seasonality and its variation between years.

The Remotely Sensed Data

We use spectral radiometric data in the visible (ocean colour) and the infra-red (SST) to construct the ecological indicators. We extracted the time series for ten representative $1^\circ \times 1^\circ$ on the continental shelf of the Northwest Atlantic Ocean (see Fig. 1). One condition used in selecting the boxes was that they should lie entirely inside the 200 m depth contour. The chlorophyll fields come from the SeaWiFS mission, reprocessing 5.2, global area coverage (Feldman and McClain 2007), level 3 binned data as presented in the Giovanni project (Acker and Leptoukh 2007). Nine apparent outliers were found in the Giovanni series. On examination of the 0.1° Giovanni data, eight outliers showed evidence of cloud-edge artifacts. They were assigned missing-value codes and new spatial means were calculated. The ninth value was accepted without change.

We also used the data from the SeaWiFS mission to develop a climatological average of photosynthetically active radiation (PAR) as a function of day number and latitude (Platt et al. 2009). Finally, we constructed time series of SST on the same scales of time and space as for chlorophyll using data from the NOAA/NASA AVHRR Pathfinder missions (Pathfinder v5.0 SST data set, JPLPO.DAAC Product #216).

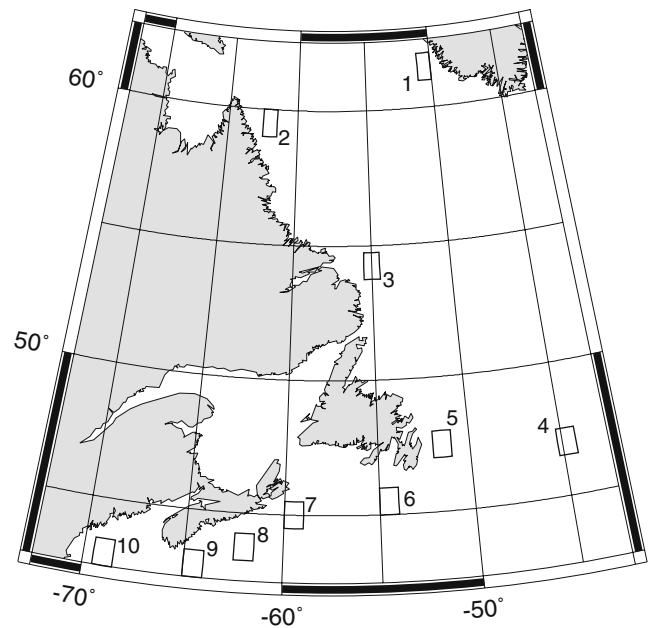


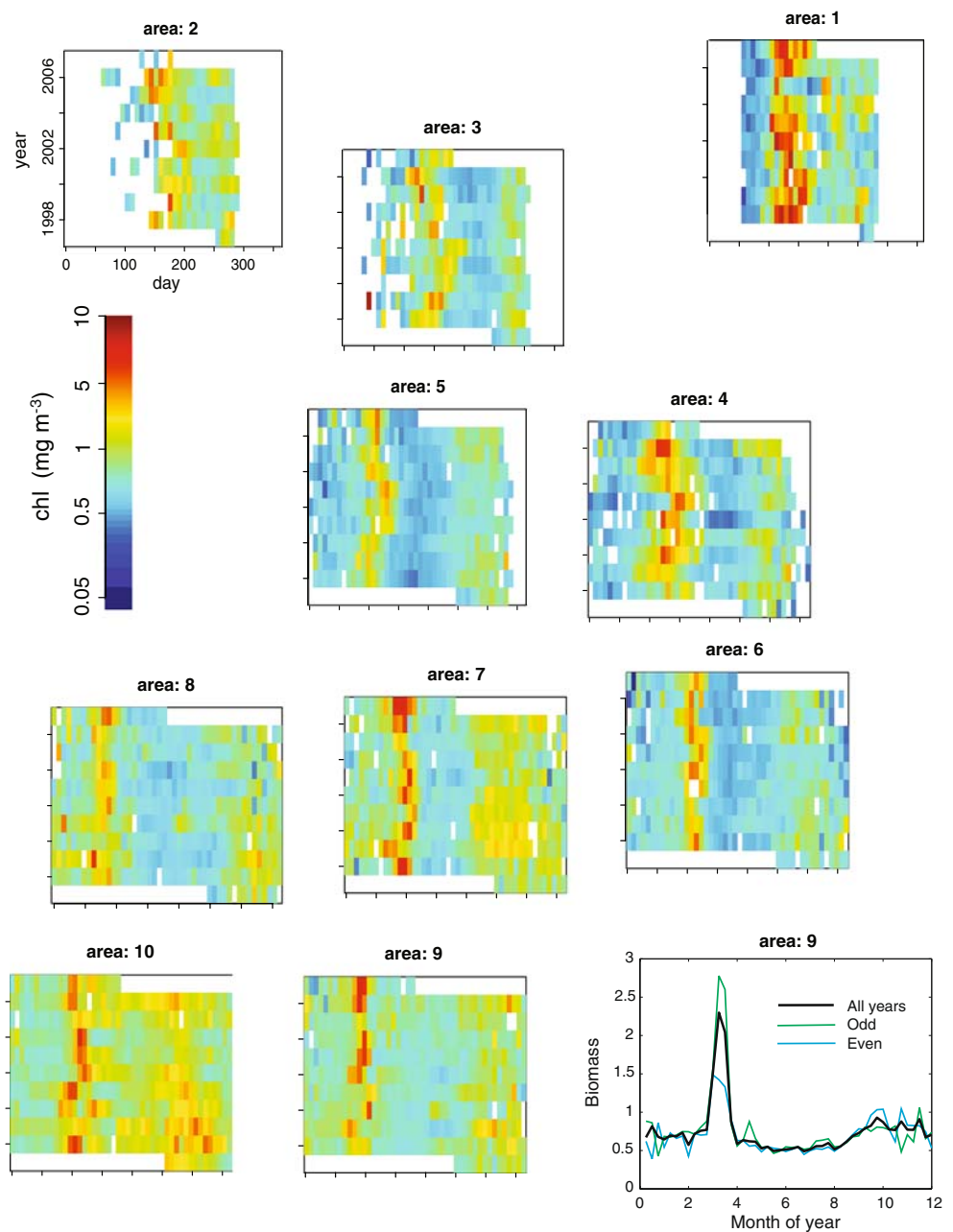
Fig. 1 Map showing the locations of the ten boxes for which time series were constructed

Ecological Indicators

The basic time series are presented in Fig. 2, using a logarithmic scale to display chlorophyll. It is clear that, for any given $1^\circ \times 1^\circ$ square, there is considerable variability within and between years. We seek to provide economical summaries of this variability by reduction of the data to a set of objective indices for each box.

The rationale for, and the approach to, development of the indicators is set out in Platt and Sathyendranath (2008). The indicators we have considered so far (Table 1) are now briefly summarised. The first four relate to the characteristics of the main event in the pelagic calendar, namely the spring bloom of phytoplankton. This phenomenon can be described with respect to its amplitude, time of initiation, time of maximum and its duration (Platt and Sathyendranath 1996; Platt et al. 2003, 2007; Rolinski et al. 2007; Cloern and Jassby 2008). The next two indicators are the parameters of the photosynthesis-light curve, which can be recovered from remotely sensed data on chlorophyll and SST using a nearest-neighbour method (Platt et al. 2008). Then, we have the phytoplankton production itself, either the annual production or the phytoplankton production integrated over the duration of the spring bloom, a first-order estimate of annual new production (Platt et al. 1992). Starting from a given chlorophyll field in a time series, we can calculate phytoplankton production and, thus, estimate the chlorophyll field at the next time step (Zhai et al. 2008). The difference

Fig. 2 Time series of chlorophyll for the ten regions, shown with approximate relative geographic positioning. For each *panel*, the ordinate represents the different years of the series and the abscissa the day numbers throughout the year. Thus, the time series for a given year can be read as the row labelled by that year. Each column shows a time series over years of biomass on a particular day number. As a further illustration, the climatology of *box 9* is shown for all years pooled and separately for odd- and even-numbered years



between this estimate and the observed field at the next time step provides an estimate of the total loss rate (grazing, sinking and so on). The loss may be integrated over any time interval, as required. The next four indicators relate to the carbon pools in the pelagic system. Particulate carbon can be estimated from chlorophyll by the method of Sathyendranath et al. (2009). Simple ecological considerations then allow estimation of carbon contained in phytoplankton. Carbon-to-chlorophyll in phytoplankton follows immediately, and because we already have the photosynthesis parameters, phytoplankton growth rate can be

recovered without difficulty. Spatial variances in the fields of biomass and production are readily calculated and are significant in many ecological contexts.

The three remaining entries in Table 1 relate to qualitative properties of the pelagic ecosystem. The first concerns the community structure of the phytoplankton. At the time of writing, it is certainly possible to diagnose the presence of diatoms (Sathyendranath et al. 2004) and to state whether the community structure at a given pixel is dominated by diatoms. The second relates to the size structure of the phytoplankton (Devred et al. 2006; Loisel et al. 2006). The last entry concerns

Table 1 Some ecological indicators for the pelagic ocean, as developed from remotely sensed spectral radiometry in the visible (ocean colour), adapted from Platt and Sathyendranath (2008)

| Indicator | Label | Dimensions |
|---|--------------|-------------------------------------|
| Initiation of spring bloom | b_i | [T] |
| Amplitude of spring bloom | b_a | [ML ⁻³] |
| Timing of spring maximum | b_t | [T] |
| Duration of spring bloom | b_d | [T] |
| Initial slope of light-saturation curve | α^B | [L ²] |
| Assimilation number | P_m^B | [T ⁻¹] |
| Total production in spring bloom | b_p | [ML ⁻²] |
| Annual phytoplankton production | P_Y | [ML ⁻²] |
| Generalised phytoplankton loss rate | L | [ML ⁻³ T ⁻¹] |
| Integrated phytoplankton loss | L_T | [ML ⁻³] |
| Particulate organic carbon | C_T | [ML ⁻³] |
| Phytoplankton carbon | C_p | [ML ⁻³] |
| Carbon-to-chlorophyll ratio | χ | Dimensionless |
| Phytoplankton growth rate | μ | [T ⁻¹] |
| Spatial variance in biomass field | σ_B^2 | [M ² L ⁻⁶] |
| Spatial variance in production field | σ_P^2 | [M ² L ⁻⁴] |
| Phytoplankton functional types | NA | NA |
| Phytoplankton size structure | s | Dimensionless |
| Delineation of biogeochemical provinces | NA | NA |

the ecological partition of the region of interest into provinces. Building on the static partition of Longhurst (1998), a procedure has now been established to delineate the borders of the provinces objectively in real time (Devred et al. 2007). This partition provides a rational template on which the other indices can be mapped, as we discuss in the next section.

Table 1 deals with indicators that can be obtained using existing ocean colour sensors. Although other indicators are possible, many, such as the attempt by Walker and Rabalais (2006) to delineate areas of coastal hypoxia, are dependent on improvements in data frequency and resolution.

Ecological Provinces

One of the advantages of the dual series of chlorophyll and SST is that they allow a partition of the region of interest (in this case, the Northwest Atlantic Ocean) into ecological provinces. This concept was introduced by Platt and Sathyendranath (1988, 1999) to provide a template for the assignment of photosynthesis parameters in calculation of phytoplankton production in a large horizontal scale. It was implemented at the global scale by Longhurst et al. (1995) and justified at length by Longhurst (1998, 2007). The boundaries between provinces are not fixed but vary with the physical forcing upon which the partition is based. The centres of mass of the provinces may move with season.

Using the remotely sensed data on SST and chlorophyll, Devred et al. (2007) have shown how to delineate the boundaries in real time. It is then possible to construct a time series of images showing the positions of the provinces and their detailed shapes, giving a picture of the adjustment of the gross ecological structure of the region as it changes with time in response to changes in the large-scale physical forcing.

The individual boxes analysed here fall into one or more of four ecological provinces, the Polar Boreal, the Arctic, the NW Atlantic Shelf, and the North Atlantic Drift, according to the partition of Devred et al. (2007). Figure 3 shows the climatological province assignment for the ten boxes over the 10-year time series. It is clear that, for the northernmost boxes (boxes 5 to 1), the province assignment is not fixed. Rather, it is variable with season. This circumstance arises in part from the condition that the boxes should all lie inside the 200-km-depth contour. As a result, the northerly boxes lie close to province boundaries. The variability is especially acute in the spring.

For example, box 1 lies mostly in the Polar Boreal province. However, in spring, the box lies sporadically

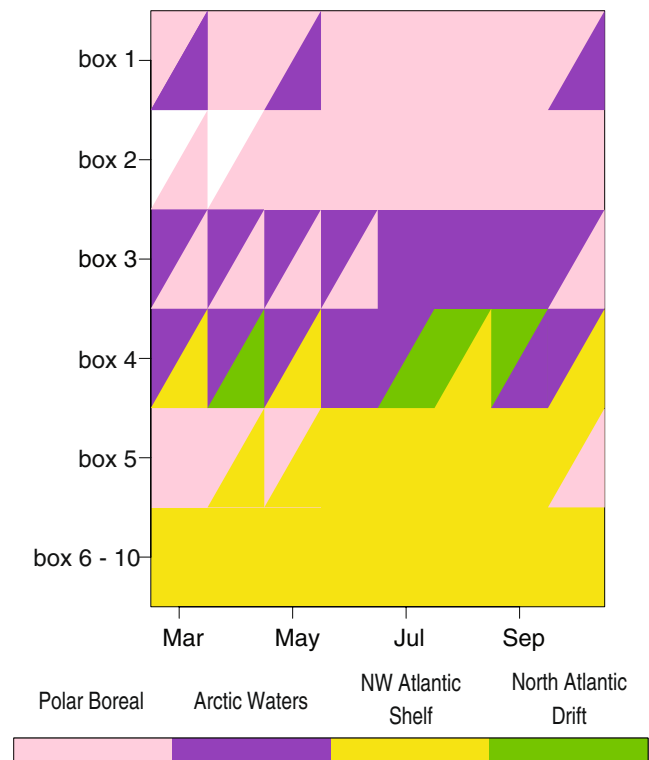


Fig. 3 Climatological assignment of boxes to biogeochemical provinces for the ten areas studied. Note that the assignments for the southerly boxes (6 to 10) are always the same, whereas this is not the case for the northerly boxes. Assignments made by the method of Devred et al. (2007)

in the Arctic province, as the forcing adjusts with season. Boxes 3 to 5, which are located at intermediate latitudes, show a high variation in the assignment of the ecological provinces. Box 3 switches between the Polar Boreal and Arctic provinces in the climatology, and box 4 is located in the Scotian Shelf province and Arctic province in spring and autumn, but lies mainly in the Arctic province and North Atlantic Drift province in the summer. These results emphasise the highly dynamic properties of the ecological provinces on a seasonal cycle and underline the value of remote sensing for tracking the variability. Boxes 6 to 10 are more stable, lying within the Scotian Shelf province during the 10-year period of observation. The variation, or otherwise, in province assignment is reflected in the dispersion of the bloom characteristics (Fig. 4).

It is clear that, before establishing a station as a site for a long-term time series, careful consideration should be given to the location of the site with respect to the boundaries of ecological provinces. Such sites ought not to be located near province boundaries. It is better to try to understand the time series as representing biological dynamics unconfounded by the seasonal migrations of province boundaries. Similarly, the representativeness of a particular study site can be judged only in reference to the seasonal variation of the province boundaries.

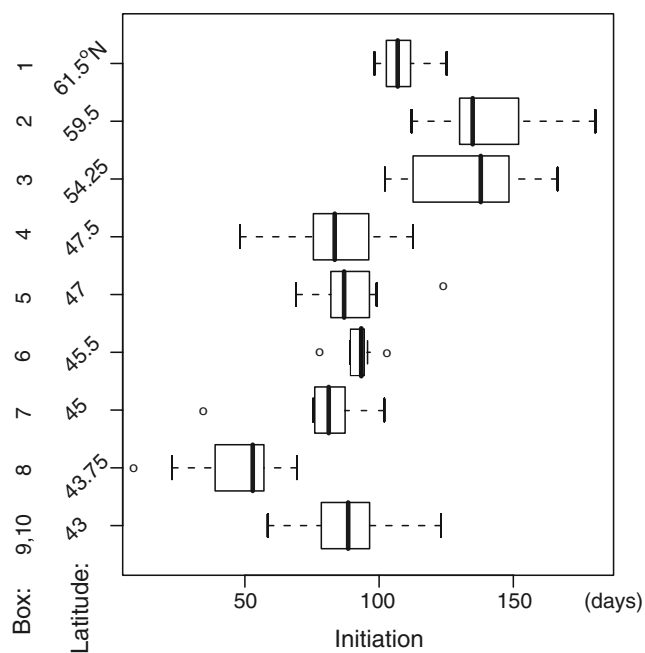


Fig. 4 Dependence of initiation times for spring and summer blooms, as obtained from fitting shifted-Gaussian curves, on latitude. Data are grouped by latitude and summarised using boxplots for the 10-year time series. For this figure, data for areas 9 and 10 were pooled

Our study in the Northwest Atlantic Ocean, in which the choice of the boxes was restricted by the bottom topography (all boxes should lie wholly on the continental shelf), has revealed instances in which temporal changes in pelagic properties (qualitative and quantitative) at a given location result from a spatial succession of ecosystems, as well as from seasonal changes within a given ecosystem. Awareness of such instances is invaluable in the interpretation of apparent anomalies in the time series. Remote sensing is an invaluable aid to making the relevant judgements.

Phenology of Phytoplankton Blooms

As is immediately evident in the time series displayed in Fig. 2, the salient feature of the pelagic ecosystem in the Northwest Atlantic Ocean is a pronounced seasonality. The stereotypical cycle includes a strong bloom in the spring and a weaker bloom in the autumn: In general, these features are clearly visible in Fig. 2. The generic mechanism for initiation of the spring bloom, as elucidated by Sverdrup (1953), is related to the rapid increase in insolation during spring, a phenomenon that is latitude-dependent. Thus, we expect the phenology of the spring bloom to vary with latitude.

What is perhaps not so expected is the high degree of variability between years in the phenology of the blooms at a given latitude, both in spring and autumn, that can be seen in Fig. 2. There is a long-standing view in the literature that such variability is of high significance to the survival of larval fish, even to the extent that year-class strength of exploited stocks might be determined by the matching (or lack of match) between bloom timing and time of spawning (Hjort 1914; Cushing 1990). Phenology of the spring bloom, as determined by serial remotely sensed data over several years, permitted an operational test of this hypothesis for a gadoid fish on the continental shelf of Nova Scotia (Platt et al. 2003, 2007), as shown in Fig. 5. The autumn bloom of phytoplankton may also play a role in the success of year classes of exploited fish (Friedland et al. 2008), and its phenology may yield further indicators of ecosystem status.

Cushing (1959) discussed seasonality in the phytoplankton as a function of latitude. His caricature of the seasonal cycle included both spring and autumn blooms in temperate latitudes, but only a single peak in the Arctic spring. He took the view that the cycle could be represented by a Lotka–Volterra system with biomass of algae and herbivores as the state variables. Subsequently, Huppert et al. (2005) have modelled seasonal phytoplankton blooms using algal biomass and

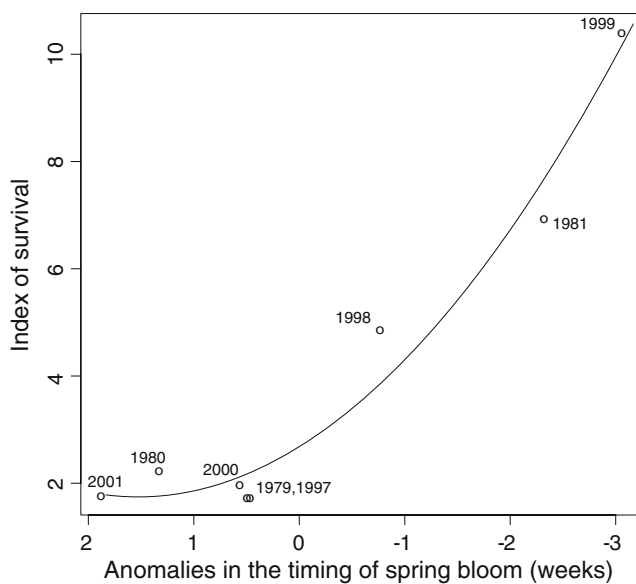


Fig. 5 Survival of larval haddock (*Melanogrammus aeglefinus*) on the continental shelf of Nova Scotia, as a function of the timing of the spring bloom (1979 to 1981 and 1997 to 2001). Larval survival is normalised to biomass of the spawning stock. Negative anomalies of bloom timing are early with respect to the climatological average. Earlier blooms are more favourable for survival of the larvae (after Platt et al. 2003)

nutrients as state variables, also in a Lotka–Volterra system. To give a context to our observations in the Northwest Atlantic Ocean, we have modelled the phytoplankton–nutrient system (Lotka–Volterra) under periodic forcing Platt et al. (2009).

The (periodic) forcing function $e(t, \theta)$, where t is the time (day number) and θ is the latitude, is the climatological average of the seasonal cycle of daily PAR in the region, developed from the SeaWiFS data series (Platt et al. 2009). It includes the decrease in amplitude of the seasonal cycle as latitude increases, and seasonally varying cloud cover. If B represents the (pigment) biomass of phytoplankton and S represents

the concentration of an essential substrate (for example, concentration of nitrate), then

$$\frac{dB}{dt} = (ae(t, \theta)S(t) - b)B(t);$$

$$\frac{dS}{dt} = (c(S_0 - S(t)) - ae(t, \theta)B(t))S(t),$$

where a , b , c and S_0 are parameters. The equations are scaled in such a way that one unit of substrate is consumed to produce one unit of biomass. We have examined the seasonal cycle of phytoplankton at different latitudes as portrayed by this simple periodic model. The model reproduces the main features of the seasonal cycle of phytoplankton biomass and its variation with latitude (Fig. 6), as anticipated qualitatively by Cushing (1959), in particular, the tendency for the autumn bloom, present in mid-latitudes, to disappear at higher latitudes. It is to be noted that the model does not follow exactly the same phase trajectories in different years at the same latitude. Although the qualitative characteristics of the cycle do not differ between years, the details of the trajectories (for example, amplitude and timing of the blooms) may vary. Also noteworthy is that the model admits solutions with a 2-year period, such that trajectories differ between even- and odd-numbered years at the same latitude (Platt et al. 2009). The differences are detectable in the observations, e.g., for box 9, Fig. 2).

The results for the phenology of the spring blooms in the representative 1° squares are given in Table 2. The expectation is that, in boxes located in higher latitudes, the bloom would tend to start later in the year. Generally speaking, this is indeed the case, but it is also clear that local considerations modify this trend. For example, the bloom begins in box 1 (West Greenland) earlier than expected from latitude alone. Again, for the three boxes located on the continental

Fig. 6 Phase plane plots showing model phytoplankton biomass (arbitrary units) and input PAR (Einsteins $m^{-2} day^{-1}$) for two latitudes. The generic model result is that there are two major peaks per year at the lower latitude, but only one at the higher latitude. Simulation results for 3 years are shown, with a different colour assigned to each year

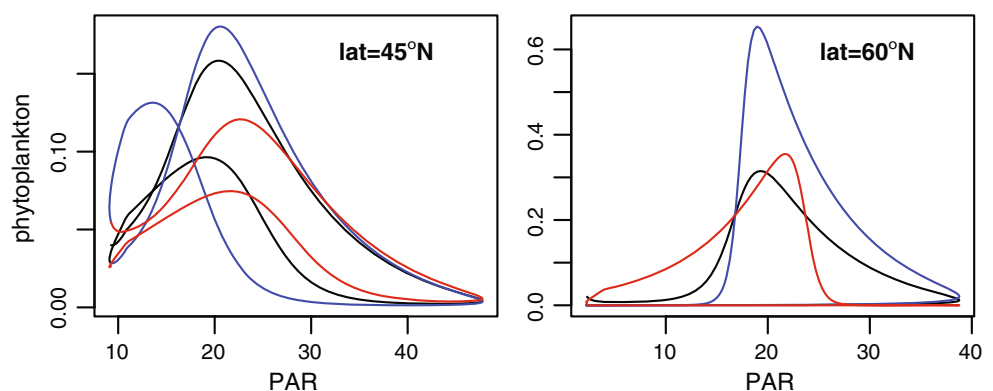


Table 2 Characteristics of spring bloom from shifted Gaussian model fitted every year to time series for each box

| | Amplitude (mg m^{-3}) | | Duration (days) | | Initiation time (day number) | | Time of peak (day number) | |
|---|-------------------------------------|------|--------------------|------|---------------------------------|------|------------------------------|------|
| | Mean | s.d. | Mean | s.d. | Mean | s.d. | Mean | s.d. |
| 1—West Greenland (50.5°W , 61.5°N) | 5.2 | 2.1 | 48 | 22 | 109 | 8 | 133 | 9 |
| 2—North Labrador (62.0°W , 59.5°N) | 2.9* | 1.5 | 65 | 25 | 142 | 26 | 175 | 21 |
| 3—Hamilton Bank (55.0°W , 54.25°N) | 2.4 | 0.8 | 39 | 13 | 134 | 22 | 153 | 19 |
| 4—Flemish Cap (45.75°W , 47.0°N) | 2.8 | 1.3 | 85 | 24 | 90 | 18 | 132 | 15 |
| 5—Grand Banks (51.5°W , 47.5°N) | 1.9 | 0.6 | 50 | 19 | 82 | 19 | 107 | 13 |
| 6—Saint Pierre Bank (54.5°W , 45.5°N) | 2.9 | 0.8 | 33 | 6 | 92 | 6 | 109 | 6 |
| 7—Banquereau Bank (59.5°W , 45.0°N) | 4.3 | 1.7 | 31 | 14 | 79 | 18 | 95 | 12 |
| 8—Western Bank (62.0°W , 43.75°N) | 2.0 | 0.5 | 59 | 29 | 47 | 19 | 76 | 7 |
| 9—Baccaro Bank (64.5°W , 43.0°N) | 4.3 | 2.1 | 24 | 9 | 80 | 13 | 92 | 10 |
| 10—Georges Bank (69.0°W , 43.0°N) | 4.2 | 1.8 | 40 | 30 | 97 | 14 | 116 | 15 |

Indicated coordinates are for the centre of each $1^\circ \times 1^\circ$ box. For all series, $n = 9$ except for area 2, where the model fit failed in 4 of the 9 cases
* ($n = 5$)

shelf off Nova Scotia (7, 8 and 9), the time of bloom initiation varies considerably, box 8 being clearly earlier than the other two. It is also the case that the timing of the spring bloom is less variable in some areas than others. For example, the timing of the spring bloom in box 6 (Grand Bank) is remarkably consistent over the 10-year series, whereas the opposite is the case for box 3 (Labrador Shelf).

Inspection of the various panels in Fig. 2 reveals variations between years in the amplitude, timing and duration of the spring blooms. It is evident that, for particular boxes, the spring bloom may be very weak in some years. The phenology and strength of the autumn bloom also vary markedly between years and between areas. Generally, the autumn bloom is a stronger feature in the lower latitudes than in the higher.

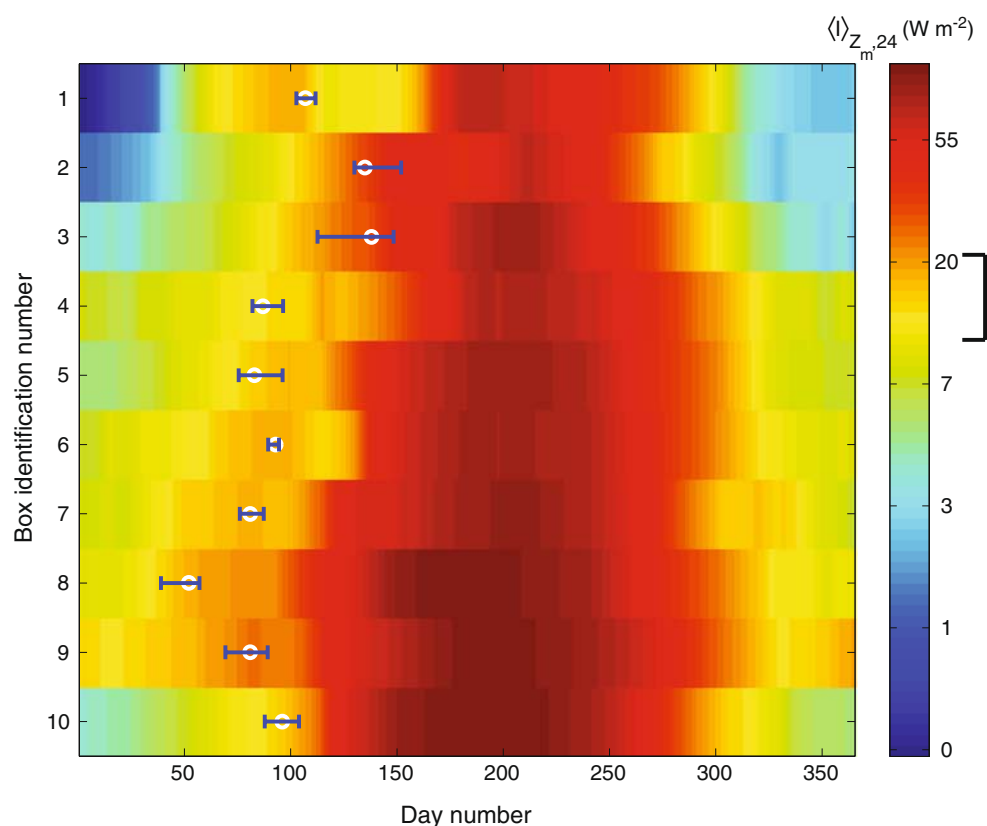
It is clear that these differences, between areas and between years, in the properties of both spring and autumn blooms of phytoplankton, will have an impact on the functioning of the whole ecosystem (for example, Platt et al. 2003; Fuentes-Yaco et al. 2007; Cloern and Jassby 2008). It is also clear that remote sensing offers the best (perhaps the only) method by which they can be established over regional scales.

It remains to reconcile the differences between the boxes with respect to the timing of bloom initiation. As discussed in Platt et al. (1991), the conventional theory is still that of Sverdrup (1953): it emphasises the shallowing of the mixed layer in the spring as the local solar intensity and day length increase. Other

factors (related to salinity) also affect stratification. Both mixed-layer depth and solar input change as the season advances, and both affect $\langle I \rangle_{Z_m,24}$, the mean irradiance in the mixed layer, averaged over the day, which is an essential property in the Sverdrup theory.

We have calculated $\langle I \rangle_{Z_m,24}$ (Fig. 7) for each of the ten boxes for every day of the year according to the 10-year climatology with mixed-layer depths calculated (as the depth at which density changes by 0.1 kg m^{-3}) from the temperature and salinity climatologies given by Tang (2007). The average light in the mixed layer lies in the range from 0 to 100 W m^{-2} . In our results, the spring bloom does not start until $\langle I \rangle_{Z_m,24}$ reaches at least 13 W m^{-2} , and $\langle I \rangle_{Z_m,24}$, on the bloom initiation day (climatological timing) is always in the range from 13 to 32 W m^{-2} (Table 3). Boxes 2 and 3 lie at the high end of this range, possibly a consequence of those boxes lying near the boundaries of their ecological province, as already discussed. Furthermore, field data on mixed-layer depth are lacking for these two boxes at the time of the bloom initiation, such that their values had to be interpolated. If we omit these two boxes, because of the relative uncertainty, the range of $\langle I \rangle_{Z_m,24}$ on bloom initiation day is only 13 to 25 W m^{-2} , with a median value of 17 W m^{-2} . Given the annual range of $\langle I \rangle_{Z_m,24}$, and considering also the difficulty of getting reliable mixed-layer depths at the appropriate time resolution, the observed range of $\langle I \rangle_{Z_m,24}$ can be seen as remarkably narrow. These results are illustrated in Fig. 7.

Fig. 7 Seasonal variation in mean irradiance in mixed layer over the day. Also marked are the mean and range of bloom initiation times for each box. The square bracket on the irradiance scale shows the range in mean irradiance in mixed layer at bloom initiation, for the eight boxes with field observations (see text)



Community Structure

In addition to providing fields of chlorophyll concentration, remote sensing of ocean colour offers the possibility of assessing the community structure of the phytoplankton, important for both food-web analyses (Cury et al. 2008) and biogeochemistry (LeQuéré et al. 2005). Phytoplankton community composition is tied to the phenology of blooms (Bruno et al. 1983), has been linked to growth rates of commercially important

bivalves (Greenfield et al. 2005) and is of interest in developing nearshore management schemes (Roelke et al. 1999). For the North Atlantic, Sathyendranath et al. (2004) developed an algorithm for detection of pixels at which the community is dominated by diatoms. At the global scale, Alvain et al. (2005) and Hirata et al. (2008) have published algorithms to determine which of four phytoplankton groups dominates the community at a particular time and location.

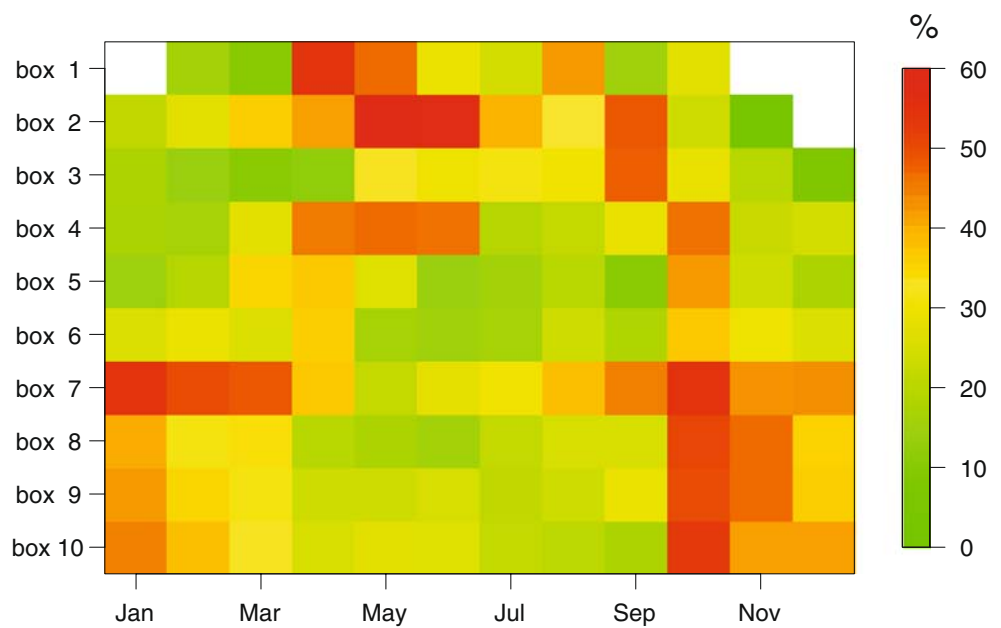
We have applied the algorithm of Sathyendranath et al. (2004) to the ocean colour time series for the ten 1° squares in the Northwest Atlantic to construct time series of the variation of diatom dominance between seasons and between years (Fig. 8). In general, there are similarities with the chlorophyll seasonalities (Fig. 2). These data allow us to examine the question: does the incidence of diatoms coincide with the outbreak of blooms (as expected from general ecological principles)? The spring bloom coincides with a high probability of occurrence of diatoms in the southerly boxes (boxes 7 to 10). The autumn bloom is also associated with the occurrence of diatoms in the same areas. The probability of the occurrence of diatoms is examined in more detail in Fig. 9 for box 7.

Diatoms tend to flourish later as latitude increases; however, diatoms may occur earlier than expected (for

Table 3 Mixed-layer depth, vertical attenuation coefficient and mean irradiance over the day, all at the time of (climatological) spring bloom initiation

| Box | Init. (day) | Z_m (m) | B (mg m^{-3}) | K_d (m^{-1}) | $\langle I_o \rangle_{24}$ (W m^{-2}) | $\langle I \rangle_{Z_m, 24}$ |
|-----|-------------|-----------|----------------------------|---------------------------|--|-------------------------------|
| 1 | 107 | 43 | 0.55 | 0.083 | 61 | 17 |
| 2 | 135 | 26 | 0.70 | 0.093 | 84 | 32 |
| 3 | 138 | 32 | 0.71 | 0.093 | 96 | 30 |
| 4 | 87 | 67 | 0.50 | 0.080 | 71 | 13 |
| 5 | 83 | 54 | 0.49 | 0.079 | 69 | 15 |
| 6 | 93 | 49 | 0.61 | 0.087 | 78 | 18 |
| 7 | 81 | 40 | 0.72 | 0.093 | 69 | 18 |
| 8 | 52 | 28 | 0.66 | 0.090 | 49 | 18 |
| 9 | 81 | 27 | 0.77 | 0.096 | 73 | 25 |
| 10 | 96 | 51 | 0.97 | 0.107 | 84 | 15 |

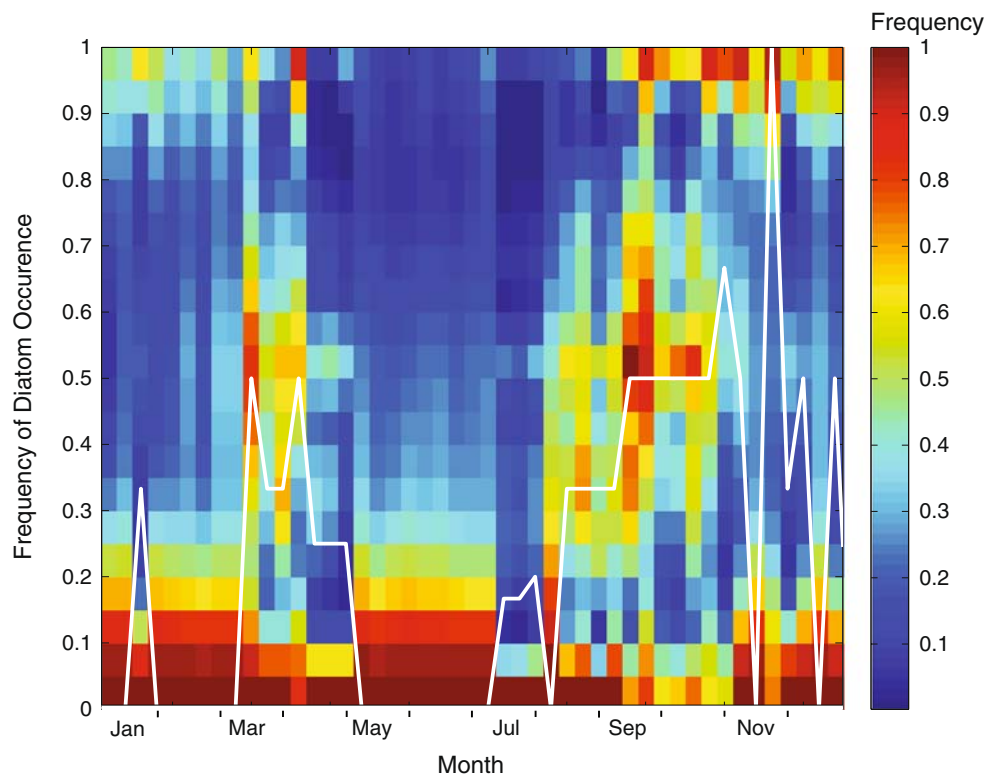
Fig. 8 The probability that the community structure of phytoplankton in the boxes is dominated by diatoms. Climatology of seasonal variation, as established using the algorithm of Sathyendranath et al. (2004)



example, in box 1), judging by latitude (Fig. 8). It is also remarkable that the period for which the probability of occurrence of diatoms is greater than 30% is longer in the southerly provinces than in the northerly provinces.

In fact, the probability of occurrence of diatoms in the northerly provinces is low in the autumn, which is consistent with the absence of phytoplankton blooms in these areas at that time of the year (Fig. 2).

Fig. 9 Seasonal variation of diatom occurrence in box 7. Colour scale refers to frequency distribution (over all pixels and years) of diatom occurrence. Solid white line is the median value of diatom occurrence over all data



Concise Descriptions of the Pelagic Ecosystem

Taken together, the ocean-colour fields and the SST fields provide an extremely rich body of information about the pelagic ecosystem and how it changes over time. However, the data flow is very heavy and the information contained therein is indigestible unless steps are taken to extract a more concise description. The first issue is to average the information over the appropriate scales of time and space. The spatial scale is usually simple to establish, as it is often implicit in the question to be addressed. However, it is worth bearing in mind where the area over which the data are to be averaged lies in relation to the ecological partition of the region in which it is embedded. It could be misleading to average over an area that covers more than one ecological province.

In selecting the time scale, the intrinsic ecological time scale relevant to the question being addressed is the principal concern. However, another issue also comes to the fore. Cloud cover reduces the availability of useful images. It is usual to combine information from two or more satellite passes to construct composite images representing conditions during the time interval over which the data are to be averaged. The longer the averaging time, the greater the chance that given pixels will not lack data because of cloud. On the other hand, longer averaging times degrade our ability to resolve events at short time scales. A compromise must be struck. In the Northwest Atlantic Ocean, we have found that a 1-week averaging is about the shortest that will provide useful information for time series. Seasonal and annual averages (or totals) will have their own applications, in the usual way.

Our analysis reveals that, in the pelagic ecosystem, for which the dominant forcing is seasonal with a periodicity of 1 year, there may be significant variance at longer time scales. This conclusion is an emergent property of the phytoplankton-nutrient model, and it is reinforced by analysis of the observations (Platt et al. 2009). Such a feature of the observations could easily have been overlooked, emphasising the utility of data analysis in the context of a simple model. Indirectly, the results of Friedland et al. (2008), that the survival of haddock larvae in 1 year may be affected by the characteristics of the autumn phytoplankton bloom in the previous year, also alert us to the reality that conventional methods for analysis of ecological time series in the ocean may not be sufficient. We are used to calculating climatologies on the assumption that the relevant time scale is 1 year. However, we should keep an open mind to the possibility that averaging at other time scales may be required (Fig. 2).

Once the averaging issues are resolved, we can proceed to construct the concise description. It is proposed that an economical description of the state of the pelagic ecosystem can be established as a vector whose elements are ecological indices selected from the options available in Table 1. The temporal development of the system can then be represented as the temporal evolution of the selected vector elements. The choice of indicators to be selected from Table 1 depends on the purpose for which the description is required. For example, if the question concerns interannual variability in the phenology of the spring bloom of phytoplankton, we might select the four descriptors of bloom characteristics as a minimal set. An extended set might include the phytoplankton production integrated over the duration of the bloom, the total loss rate integrated through the bloom, the spatial variances in biomass and production during the bloom, and relative dominance of diatoms. Even the extended set would represent a remarkably concise, but at the same time objective and highly informative, synthesis of a massive body of information.

The international consensus to manage marine resources on an ecosystem basis has created a requirement for objective indicators of the ocean ecosystem. We have seen that, as far as the pelagic ecosystem is concerned, remote sensing is a direct avenue to the construction of pertinent indicators (Platt and Sathyendranath 2008). As operational oceanography becomes established as an activity in its own right, the demand for such indicators can only increase. It will be important to insist that their application in the operational community should not be separated from the research environment in which they were developed. The range of indicators available should be extended and refined through close interaction between research and operational communities, and their collective utility tested in the crucible of the decision-making user community. One should also not lose sight of the fact that, notwithstanding the striking beauty of ocean-colour images, the basic information that lies behind them is based on the most rigorous radiometric science. To interpret the data to the fullest extent requires expertise in radiative transfer and bio-optics, and such input will always be required to develop the most refined interpretation of phytoplankton time series as observed by remote sensing.

The remotely sensed data required to develop pelagic indicators highly resolved in space and time have been available in a reliable stream only since 1997, that is to say some 10 years at the time of writing. In the early 1990s, when major fisheries collapsed in the Northwest Atlantic with irreparable damage to the

social fabric, it was not possible, for want of suitable data, to assess the extent to which ecosystem variability was a contributing factor. Fortunately, we now have much of the data we need from remote sensing, and serial indicators of the pelagic ecosystem should make a constructive contribution to discussions of similar problems in the future. Improvements in both spectral and spatial resolution will broaden the range of possible applications in coastal waters. Most importantly, if the time series, and the indicators derived therefrom, are to be of the highest value, it is essential that continuity be maintained in the ocean-colour data stream.

References

- Acker, J.G., and G. Leptoukh. 2007. Online analysis enhances use of NASA Earth Science data. *Eos, Trans. AGU* 88: 14, 17.
- Alvain, S., C. Moulin, Y. Dandonneau, and F.M. Bréon. 2005. Remote sensing of phytoplankton groups in case 1 waters from global SeaWiFS imagery. *Deep-Sea Research I* 52: 1989–2004.
- Bruno, S.F., R.D. Staker, G.M. Sharma, and J.T. Turner. 1983. Primary productivity and phytoplankton size fraction dominance in a temperate North Atlantic estuary. *Estuaries* 6(3): 200–211.
- Cloern, J.E., and A.D. Jassby. 2008. Complex seasonal patterns of primary producers at the land-sea interface. *Ecology Letters* 11(12): 1294–1303.
- Cury, P., Y.-J. Shin, B. Planque, J. Durant, J.-M. Fromentin, S. Kramer-Schadt, N. Stenseth, M. Travers, and V. Grimm. 2008. Ecosystem oceanography for global change in fisheries. *Trends in Ecology and Evolution* 23: 338–346.
- Cushing, D.H. 1959. The seasonal variation in oceanic production as a problem in population dynamics. *Journal du Conseil* 24(3): 455–464.
- Cushing, D.H. 1990. Plankton production and year-class strength in fish populations: An update of the match/mismatch hypothesis. *Advances in Marine Biology* 26: 249–294.
- Devred, E., S. Sathyendranath, and T. Platt. 2007. Delineation of ecological provinces in the North West Atlantic using visible spectral radiometry (ocean colour). *Marine Ecology Progress Series* 346: 1–13.
- Devred, E., S. Sathyendranath, V. Stuart, H. Maass, O. Ulloa, and T. Platt. 2006. A two-component model of phytoplankton absorption in the open ocean: Theory and applications. *Journal of Geophysical Research* 111: C03011. doi:10.1029/2005JC002880.
- Feldman, G.C., and C.R. McClain. 2007. Ocean color web, SeaWiFS reprocessing 5.2. Greenbelt: NASA Goddard Space Flight Center.
- Friedland, K., J.A. Hare, G. Wood, L. Col, L. Buckley, D. Mountain, J. Kane, J. Brodziak, R.G. Lough, and C.H. Pilskaln. 2008. Does the fall phytoplankton bloom control recruitment of Georges Bank haddock, *Melanogrammus aeglefinus*, through parental condition? *Canadian Journal of Fisheries and Aquatic Sciences* 65(6): 1076–1086.
- Fuentes-Yaco, C., P.A. Koeller, S. Sathyendranath, and T. Platt. 2007. Shrimp (*Pandalus borealis*) growth and timing of the spring phytoplankton bloom on the Newfoundland-Labrador Shelf. *Fisheries Oceanography* 16(2): 116–129.
- Greenfield, D., D.J. Lonsdale, and R.M. Cerrato. 2005. Linking phytoplankton community composition with juvenile-phase growth in the Northern Quahog *Mercenaria mercenaria* (L.). *Estuaries and Coasts* 28(2): 241–251.
- Hirata, T., J. Aiken, N. Hardman-Mountford, T. Smyth, and R. Barlow. 2008. An absorption model to determine phytoplankton size classes from satellite ocean colour. *Remote Sensing of Environment* 112(6): 3153–3159.
- Hjort, J. 1914. Fluctuations in the great fisheries of Northern Europe, viewed in the light of biological research. *Const. Int. Explor. Mer.* 20: 1–228.
- Huppert, A., B. Blasius, R. Olinky, and L. Stone. 2005. A model for seasonal phytoplankton blooms. *Journal of Theoretical Biology* 236: 276–290.
- LeQuéré, C., S.P. Harrison, I.C. Prentice, E.T. Buitenhuis, O. Aumont, L. Bopp, H. Claustre, L. C. da Cunha, R. Geider, X. Giraud, C. Klaas, K.E. Kohfeld, L. Legendre, M. Manizza, T. Platt, R.B. Rivkin, S. Sathyendranath, J. Uitz, A.J. Watson, and D. Wolf-Gladrow. 2005. Ecosystem dynamics based on plankton functional types for global ocean biogeochemistry models. *Global Change Biology* 11: 2016–2040.
- Loisel, H., J.M. Nicolas, A. Sciandra, D. Stramski, and A. Poteau. 2006. Spectral dependency of optical backscattering by marine particles from satellite remote sensing of the global ocean. *Journal of Geophysical Research* 111: (C09024). doi:10.1029/2005JC003367.
- Longhurst, A. 1998. *Ecological geography of the sea*. San Diego: Academic.
- Longhurst, A. 2007. *Ecological Geography of the Sea* (2nd edn.). Amsterdam: Elsevier.
- Longhurst, A., S. Sathyendranath, T. Platt, and C. Caverhill. 1995. An estimate of global primary production in the ocean from satellite radiometer data. *Journal of Plankton Research* 17(6): 1245–1271.
- Platt, T., D.F. Bird, and S. Sathyendranath. 1991. Critical depth and marine primary production. *Proceedings of the Royal Society of London, Series B: Biological Sciences* 246: 205–217.
- Platt, T., C. Fuentes-Yaco, and K.T. Frank. 2003. Spring algal bloom and larval fish survival. *Nature* 423: 398–399.
- Platt, T., P. Jauhari, and S. Sathyendranath. 1992. The importance and measurement of new production. In *Primary productivity and biogeochemical cycles in the sea*, eds. P.G. Falkowski, and A.D. Woodhead, 273–284. New York: Plenum.
- Platt, T., and S. Sathyendranath. 1988. Oceanic primary production: Estimation by remote sensing at local and regional scales. *Science* 241: 1613–1620.
- Platt, T., and S. Sathyendranath. 1996. Biological oceanography and fisheries management. *Int. Counc. Explor. Sea* CM 0: 3.
- Platt, T., and S. Sathyendranath. 1999. Spatial structure of pelagic ecosystem processes in the global ocean. *Ecosystems* 2: 384–394.
- Platt, T., and S. Sathyendranath. 2008. Ecological indicators for the pelagic zone of the ocean from remote sensing. *Remote Sensing of Environment* 112(8): 3426–3436.
- Platt, T., S. Sathyendranath, M.-H. Forget, G.N. White III, C. Caverhill, H. Bouman, E. Devred, and S. Son. 2008. Operational mode estimation of primary production at large geographical scales. *Remote Sensing of Environment* 112(8): 3437–3448.
- Platt, T., S. Sathyendranath, and C. Fuentes-Yaco. 2007. Biological oceanography and fisheries management: Perspective after ten years. *ICES Journal of Marine Science* 64(5): 863–869.
- Platt, T., G. N. White III, L. Zhai, S. Sathyendranath, and S. Roy. 2009. The phenology of phytoplankton blooms: Ecosys-

- tem indicators from remote sensing. *Ecological Modelling*. doi:10.1016/j.ecolmodel.2008.11.022.
- Roelke, D.L., P.M. Eldridge, and L.A. Cifuentes. 1999. A model of phytoplankton competition for limiting and nonlimiting nutrients: Implications for development of estuarine and nearshore management schemes. *Estuaries* 22(1): 92–104.
- Rolinski, S., H. Horn, T. Petzoldt, and L. Paul. 2007. Identifying cardinal dates in phytoplankton time series to enable the analysis of long-term trends. *Oecologia* 153: 997–1008.
- Sathyendranath, S., V. Stuart, A. Nair, K. Oka, T. Nakane, H. Bouman, M.-H. Forget, H. Maass, and T. Platt. 2009. Carbon-to-chlorophyll ratio and growth rate of phytoplankton in the sea. *Marine Ecology-Progress Series*. doi:10.3354/meps07998.
- Sathyendranath, S., L. Watts, E. Devred, T. Platt, C. Caverhill, and H. Maass. 2004. Discrimination of diatoms from other phytoplankton using ocean-colour data. *Marine Ecology Progress Series* 272: 59–68.
- Sverdrup, H.U. 1953. On conditions for the vernal blooming of phytoplankton. *Journal du Conseil* 18(3): 287–295.
- Tang, C. 2007. High-resolution monthly temperature and salinity climatologies for the northwestern North Atlantic Ocean. *Canadian Data Report of Hydrography and Ocean Sciences* 169: iv + 55.
- Walker, N.D., and N.N. Rabalais. 2006. Relationships among satellite chlorophyll a, river inputs, and hypoxia on the Louisiana Continental shelf, Gulf of Mexico. *Estuaries and Coasts* 29(6B): 1081–1093.
- Zhai, L., T. Platt, C.L. Tang, M. Dowd, S. Sathyendranath, and M.-H. Forget. 2008. Estimation of phytoplankton loss rate by remote sensing. *Geophysical Research Letters* 35: L23606. doi:10.1029/2008GL035666.